

Original Research

Kinetic, Isotherm and Thermodynamic Studies on the Adsorption Behavior of Atrazine onto Sheep Manure-Derived Biochar

Yixin Lu^{1,2}, Jiao Chen^{1,2}, Jianqiang Zhang^{1*}, Chenchen Fu¹

¹Faculty of Geosciences and Environmental Engineering, Southwest Jiaotong University, Chengdu, China

²Department of Architectural and Environmental Engineering, Chengdu Technological University, Chengdu, China

Received: 7 May 2018

Accepted: 5 July 2018

Abstract

Experimental and theoretical studies have been conducted to investigate the adsorption of atrazine in aqueous solutions by sheep manure-derived biochar synthesized at 650°C (SMB650). The results of characterization analysis showed that SMB650 possessed large specific surface area and was rich in pore structure and functional groups. The removal efficiency of atrazine by SMB650 was 95.3% under the optimum conditions, of which contact time, initial atrazine concentration, initial solution pH, SMB650 dosage and temperature were 150 min, 1500 µg/L, 3.0, 1.6 g/L and 25°C, respectively. The results of kinetic and isotherm studies revealed that the pseudo second-order and the Freundlich model fit the experimental data best ($R^2 > 0.98$). The adsorption of atrazine onto SMB650 belonged to multi-molecular layer adsorption. The calculated thermodynamic parameters like free energy change (ΔG^θ), enthalpy change (ΔH^θ) and entropy change (ΔS^θ) were -7.8730 to -6.2976 kJ/mol, 17.2179 kJ/mol and 0.0788 kJ/(mol·K), respectively, indicating that the adsorption process of atrazine onto SMB650 was spontaneous, endothermic and entropy-increased. The present study showed that the sheep manure-derived biochar could be used as a promising adsorbent for the removal of atrazine from aqueous solutions.

Keywords: atrazine adsorption; kinetics; isotherms; thermodynamics; sheep manure-derived biochar

Introduction

Atrazine (2-chloro-4-[ethylamino]-6-[isopropylamino]-s-triazine) is a selective herbicide that has been widely used worldwide due to its low cost and good weeding effect. However, owing to the characteristics such as stable chemical structure, superficial mobility, long

half-life and high leaching potential, atrazine has been frequently detected in the surface and ground water in many countries and regions [1-3]. Continuous exposure to atrazine may inhibit the growth of plants and animals. Moreover, atrazine can be absorbed and accumulated by the human body through food chain enrichment, which would disrupt the endocrine systems, alter immune response, retard sexual and embryo development and induce the mammary gland or cancer [4, 5]. Therefore, the removal of atrazine from water

*e-mail: zhjqicn@swjtu.cn

has been considered a significant and urgent issue in wastewater treatment.

At present, the main methods to remove atrazine include adsorption [6-9], UV and UV/MW photolysis [10], ozonation [11] and Fenton-like process [12]. Among these methods, adsorption is favored by researchers because of its advantages such as low cost, high efficiency and simple operation. Biochar is the product of biomass by pyrolysis and carbonization under oxygen-limited conditions. It possesses high specific surface area, rich pore structure and abundant functional groups, which together have led to its great adsorption potential [13-15]. Recently, a variety of biochars have been reported to apply to the removal of atrazine from aqueous solutions. Wang et al. [8] prepared wheat straw-derived biochar (WS750) via pyrolysis at 750°C and found that the sorption quantity of atrazine by WS750 could reach 12.0 mg/g. Tan et al. [16] obtained corn-straw biochar via slow pyrolysis at 500°C and suggested that its maximum sorption capacity for atrazine was 1.94 mg/g. Zhang et al. [17] reported that the sludge biochars prepared at 400°C for 2 hours had the greatest atrazine adsorption and the adsorption equilibrium time was about 36 hours. However, most research concerning the adsorption of atrazine has been limited to biochars prepared by plant residues or excess sludge. Studies on biochars derived from livestock manure for atrazine adsorption have rarely been reported. Currently, sheep farming has developed rapidly in many countries, including Poland, India and China. The amount of sheep manure increased sharply with increasing numbers of sheep. It will pose great pressure on the ecological environment if sheep manure cannot be effectively treated or reused [18-20]. Although sheep manure contains a certain amount of fertilizer, when it is not fermented, the utilization rate of the plant is low, and it is easy to cause the plant to burn roots and seedlings. Moreover, the germs, worm eggs and parasites in sheep manure may also cause the spread of diseases and insect pests. Thus, sheep manure is not suitable for direct use as fertilizer in the soil. If the sheep manure can be used to produce biochar to adsorb atrazine, it will only reduce environmental pollution but also achieve waste recycling.

In this study, the adsorption ability of biochar produced from sheep manure to atrazine from aqueous solutions was investigated. The physicochemical properties of sheep manure-derived biochar were characterized. The main factors (initial solution pH, biochar dosage, contact time, initial atrazine concentration and temperature) that affect adsorption effect were evaluated using batch experiments. Based on this, the adsorption mechanism was analyzed by kinetic, isothermic and thermodynamic models. The purpose of this study was to develop an innovative, efficient, low-cost and environmentally friendly adsorbent for the removal of atrazine from wastewater and provide a theoretical basis for the resource utilization of sheep manure.

Materials and Methods

Reagents and Chemicals

Atrazine (with purity >97%, Fig. 1) procured from Aladdin Chemical Reagent Co. Ltd, was used in the present experiment. Certain amount of atrazine was dissolved in deionized water to prepare 20 mg/L stock solution. The stock solution was diluted based on the experimental needs. The initial pH of atrazine solution was adjusted by adding 0.1 mol/L NaOH or 0.1 mol/L HCl solutions. All the chemical reagents involved were analytically pure and the water was deionized.

Preparation of Adsorbent

The sheep manure was collected from a farm in Hongya County, Sichuan Province, China. The manure was processed by a pulverizer and ground through a 60 mesh sieve after drying and picking out impurities. We dried the sifted material in an 85°C oven to a constant weight and took an appropriate amount to the crucible, and then put it into the muffle furnace after compacting and covering. It was then heated up to 650°C at a rate of 20°C/min and maintained constant temperature for 180 min before shutting down the muffle furnace and removing the pyrolysis products after cooling to room temperature. To remove the ash of the pyrolysis products, 200 mL HCl solution of 1.0 mol/L was added to 10 g pyrolysis products, the solution was oscillated at 150 r/min for 30 min and repeated three times. The products were sifted and dried in a 105°C oven to a constant weight after water washing to neutral. The sheep manure-derived biochar (SMB650) was successfully prepared after the products were cooled and passed through a 100-mesh sieve.

Adsorption Experiments

Batch experiments were conducted in the present study. In each experiment, a 50-mL atrazine solution of a certain mass concentration was placed in a 100-mL conical flask. A certain quantity of SMB650 was added and the initial solution pH value was then adjusted, and magnetic stirring was used to accelerate the

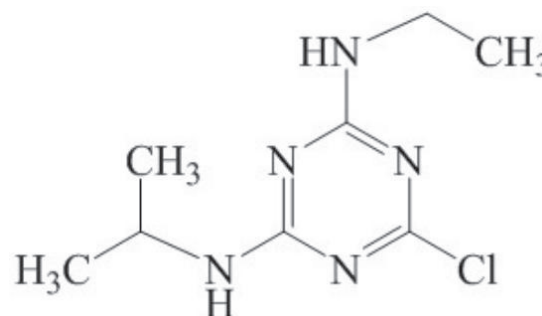


Fig. 1. Molecular structure of atrazine.

equilibrium in the adjustment process. The suspension was oscillated at 150 r/min for a certain period of time. The pH value of the solution was regularly detected during the experiment, and was kept constant by adding 0.1 mol/L HCl or NaOH. After the oscillation was over, the suspension was centrifuged at 4000 r/min for 10min and then filtered through a 0.45- μm filter membrane. The filtrate was used to analyze for the residual atrazine.

Analysis Methods

The C, H, N and O contents of SMB650 were tested by elemental analyzer (VARIO EL cube, Elementar, Germany). The specific surface area (SSA), total pore volume (TPV) and average pore diameter (APD) of SMB650 were tested by specific surface area analyzer (NOVA4000e, Quantachrome, America). The surface topography characteristics of SMB650 were tested by a field emission scanning electron microscope (SUPRA40, ZEISS, Germany). The surface functional groups of SMB650 were tested by a Fourier infrared spectrometer (FTIR Spectrum100, Perkin Elmer, America). The concentration of atrazine was tested by high-performance liquid chromatography (Waters 2695-2996, Alliance, America). The analysis was run at 225 nm using methanol: water (60: 40, v/v) as mobile phase with a flow velocity of 0.8 mL/min and a column temperature of 40°C.

The removal efficiency (η , %) and adsorption amount (q_t , $\mu\text{g/g}$) of atrazine adsorbed onto SMB650 in each test were evaluated using the following equations:

$$\eta = (C_0 - C_e) \times 100\% / C_0 \quad (1)$$

$$q_t = (C_0 - C_e)V / m \quad (2)$$

...where C_0 ($\mu\text{g/g}$) is the initial concentration of atrazine, C_e ($\mu\text{g/g}$) is the equilibrium concentration of atrazine, V (mL) is the volume of suspension, m (g) is the mass of SMB650 and t (min) is the contact time.

Results and Discussion

Physicochemical Properties of SMB650

Elemental analyses (Table 1) showed that the elemental content of SMB650 decreased in the order $\text{C} > \text{O} > \text{N} > \text{H}$. Generally, the ratios of H/C, O/C and (O+N)/C are recognized as indices for the aromaticity and polarity of adsorption materials [21, 22]. In the present study, the relatively lower ratios of H/C, O/C and (O+N)/C indicated that SMB650 was of high aromaticity and stability. Besides, the SSA, TPV and APD of SMB650 was 189.35 m^2/g , 0.252 cm^3/g and 12.43 nm, respectively. The result of SEM analysis (Fig. 2) also showed that SMB650 had rough texture with uneven surface and a large number of irregular pores. The large

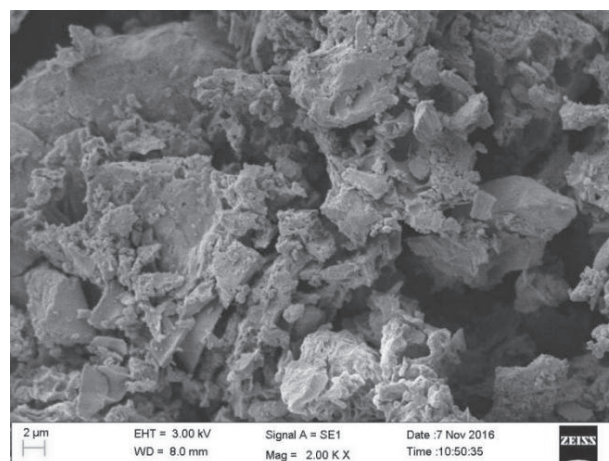


Fig. 2. SEM image of SMB650.

specific surface area and pore structure provided good conditions for atrazine adsorption onto SMB650.

The FTIR spectrogram of SMB650 is shown in Fig. 3. It can be seen that the stretching vibration of hydroxyl groups (-OH), C-H, aromatic ring (C=C and C=O) and C-O appeared at 3409 cm^{-1} , 2920 cm^{-1} , 1603 cm^{-1} and 1088 cm^{-1} , respectively, and the bending vibration of C-H appeared at 795 cm^{-1} . The result showed that the surface of SMB650 contained rich functional groups and aromatic structures, which provided a good basis for the adsorption of atrazine.

Preliminary Adsorption Studies

Effect of Initial Solution pH

The solution pH not only influences the physicochemical properties of the adsorbent but also affects the charge of adsorbate presented in the solution [23-25]. The effect of initial solution pH on the adsorption of atrazine onto SMB650 was studied using 1500 $\mu\text{g/L}$ atrazine concentration under the condition

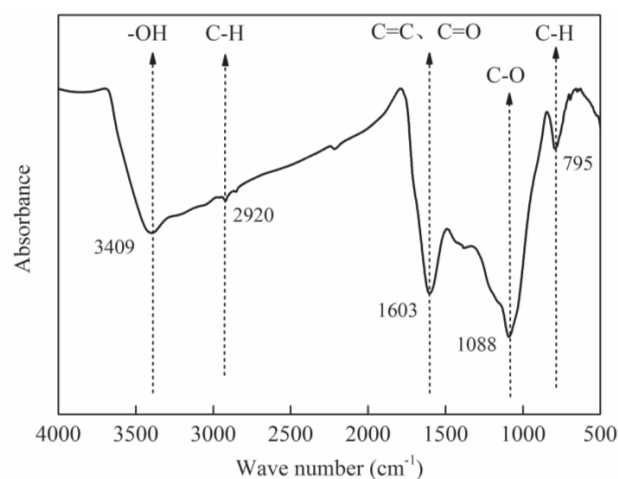


Fig. 3. FTIR spectra of SMB650.

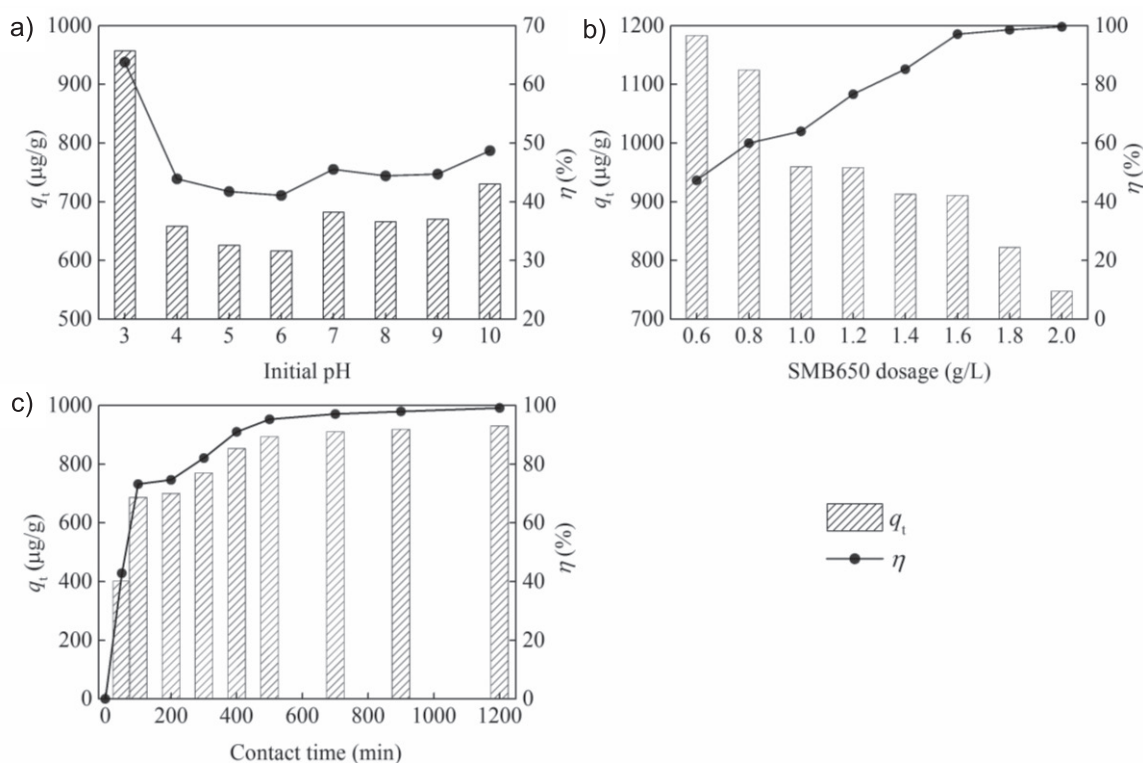


Fig. 4. Effects of different variables on adsorption efficiency: a) initial solution pH; b) SMB650 dosage; c) contact time.

of 1.0 g/L SMB650 dosage, pH 3.0-10.0 at 25°C (Fig. 4a). It should be noted that in order to avoid the dilution caused by the excessive addition of HCl or NaOH when the pH of the solution was adjusted, and to save the cost of HCl or NaOH dosage, the solution pH in this study was investigated from 3.0 to 10.0.

As can be seen, SMB650 showed the best adsorbing effect when the pH value was 3.0, with the adsorption amount of atrazine up to 957.019 $\mu\text{g/g}$ and the removal efficiency up to 63.8%. Comparatively speaking, the removal efficiency showed a 55.4% decrease when pH value was 6.0. On the one hand, since atrazine was a weakly alkaline substance its solubility decreased with the increase of pH value, and acidic condition was more favorable for adsorption. On the other hand, the atrazine was mainly in molecular form in solution when the pH value was near or less than its acid dissociation constant ($pK_a = 1.68$). Because the adsorption of atrazine was mainly carried out by proton carboxyl group and molecular morphology, the adsorption reached a maximum when the initial solution pH value was 3.0.

Effect of Biochar Dosage

One of the parameters that significantly affect adsorption capacity is the dosage of adsorbent [26]. The effect of SMB650 dosages on the adsorption capacity was studied by contacting 50 mL of atrazine solution (1500 $\mu\text{g/L}$) for SMB650, keeping the contact time for 700 min at 25°C with the optimum pH of 3.0.

A different amount of SMB650 (0.6-2.0 g/L) was added and the results are shown in Fig. 4b).

It was obvious that the removal efficiency of atrazine increased with the increase of SMB650 dosage. For instance, the removal efficiency of atrazine was up to 99.7% when the SMB650 dosage was 2.0 g/L. On the contrary, the adsorption capacity of SMB650 for atrazine decreased with the increase of the biochar dosage. When the SMB650 dosage increased from 0.6 to 2.0 g/L, the adsorption amount of atrazine decreased from 1183.133 to 747.375 $\mu\text{g/g}$. The removal efficiency was lower when the biochar amount was insufficient to adequately adsorb atrazine. Nevertheless, the excessive amount of biochar could result in spare adsorption sites, leading to the adsorption capacity decreasing because the biochar could not be fully utilized. Taking the removal efficiency, adsorption capacity and economical efficiency into overall consideration, the optimum SMB650 dosage for follow-up experiments was set to be 1.6 g/L. Under this condition, the adsorption amount of atrazine onto SMB650 was 910.603 $\mu\text{g/g}$ and the removal efficiency of atrazine was 97.1%.

Effect of Contact Time

Contact time is one of the key parameters in the adsorption process [27]. In the present study, contact time ranged from 50 to 1200 min. Other experimental parameters were 1500 $\mu\text{g/L}$ atrazine, pH 3.0, SMB650 dosage 1.6 g/L and temperature 25°C. The results of contact time affect are shown in Fig. 4c).

Table 1. Basic characteristics of SMB650.

Parameter	Value	
Yield (%)	42.86	
Ash content (%)	19.65	
Elemental analysis (%)	C	64.73
	H	1.92
	O	10.64
	N	2.41
Atomic ratio	H/C	0.030
	O/C	0.164
	(O+N)/C	0.202
SSA (m ² /g)	189.35	
TPV (cm ³ /g)	0.252	
APD (nm)	12.43	

It could be seen that the adsorption of atrazine onto SMB650 consisted of three stages: rapid adsorption (50-100 min), slow diffusion (100-500 min) and adsorption equilibrium (500-1200 min). In the rapid adsorption stage, the adsorption sites of the biochar were abundant and the adsorption rate was very high. The removal efficiency of atrazine was up to 73.2% at the end of this stage. As the contact time prolonged, atrazine began to slowly spread to the internal pores of biochar and the adsorption rate gradually slowed. When the contact time was further extended, the

remaining atrazine concentration in the solution was low and the mass transfer power was weak, so the adsorption was gradually approaching equilibrium. Hence, 500 min was considered as the optimal adsorption time. The adsorption amount of atrazine at this experimental time was 893.538 $\mu\text{g/g}$ and removal efficiency was 95.3%.

Adsorption Kinetics

To better analyze the behavior of atrazine adsorption onto SMB650, the adsorption of different initial atrazine concentrations (1500, 2000 and 2500 $\mu\text{g/L}$) were studied. The adsorption data were simulated using the pseudo first-order, pseudo second-order, intra-particle diffusion and Elovich models. The equations can be described as follows:

$$\text{Pseudo first-order model: } \ln(q_e - q_t) = \ln q_e - k_1 t \quad (3)$$

$$\text{Pseudo second-order model: } t/q_t = t/q_e + 1/k_2 q_e^2 \quad (4)$$

$$\text{Intra-particle diffusion model: } q_t = k_3 t^{1/2} + C \quad (5)$$

$$\text{Elovich model: } q_t = (1/\beta) \ln(\alpha \cdot \beta) + (1/\beta) \ln(t) \quad (6)$$

...where q_e ($\mu\text{g/g}$) and q_t ($\mu\text{g/g}$) are the adsorption amount at equilibrium and time t (min), respectively; k_1 (min^{-1}), k_2 [$\text{g}/(\mu\text{g}\cdot\text{min})$] and k_3 [$\mu\text{g}/(\text{g}\cdot\text{min}^{0.5})$] are the rate constant of pseudo first-order, pseudo second-order

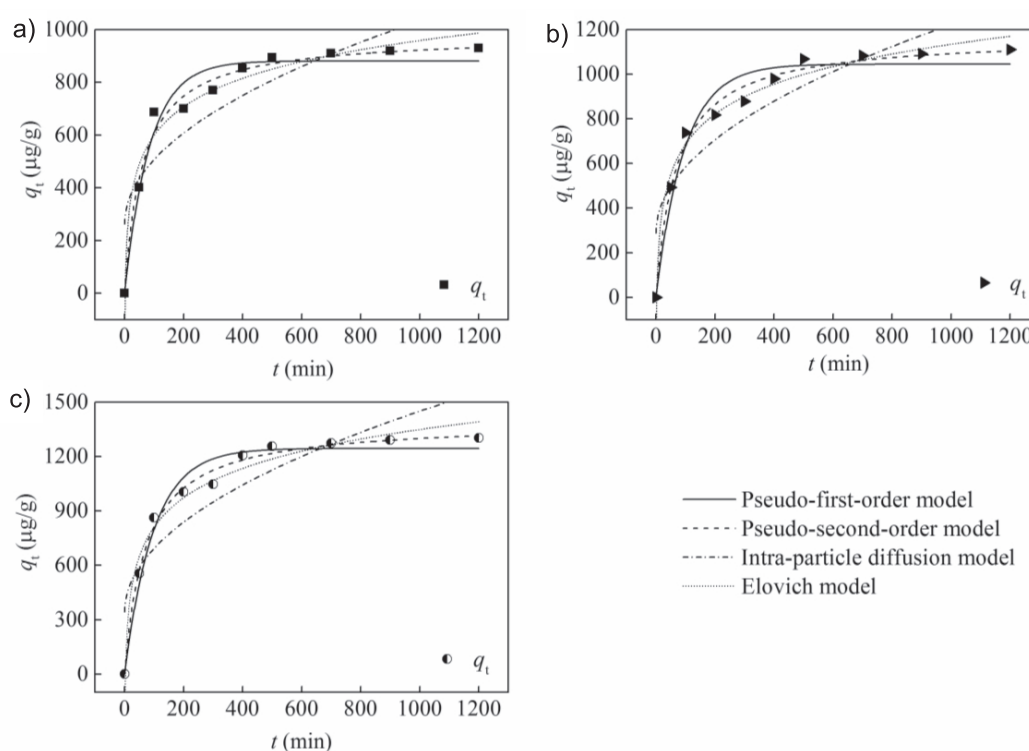


Fig. 5. Kinetic curves of atrazine adsorption onto SMB650 (initial atrazine concentration: a) 1 500 $\mu\text{g/L}$; b) 2 000 $\mu\text{g/L}$; c) 2 500 $\mu\text{g/L}$).

Table 2. Kinetic parameters for the adsorption of atrazine onto SMB650.

Kinetic model	Parameter	Initial atrazine concentration ($\mu\text{g/L}$)		
		1 500	2 000	2 500
Pseudo-first-order	q_e ($\mu\text{g/g}$)	880.690	1 044.792	1 244.399
	k_1 (min^{-1})	0.0118	0.0104	0.0103
	R^2	0.9599	0.9554	0.9713
Pseudo-second-order	q_e ($\mu\text{g/g}$)	979.500	1 169.103	1 392.681
	k_2 [$\mu\text{g}/(\mu\text{g}\cdot\text{min})$]	1.644×10^{-5}	1.216×10^{-5}	1.003×10^{-5}
	R^2	0.9819	0.9875	0.9918
Intra-particle diffusion	C	262.9421	288.1795	343.1212
	k_3 [$\mu\text{g}/(\text{g}\cdot\text{min}^{0.5})$]	24.3687	29.5518	35.0069
	R^2	0.7530	0.7988	0.7835
Elovich	A [$\text{g}/(\mu\text{g}\cdot\text{min})$]	72.0636	65.9733	74.8001
	β ($\text{g}/\mu\text{g}$)	0.0064	0.0051	0.0043
	R^2	0.9675	0.9835	0.9773

and intra-particle diffusion model, respectively; C is the boundary layer thickness; and α [$\text{g}/(\mu\text{g}\cdot\text{min})$] and β ($\text{g}/\mu\text{g}$) are the Elovich rate constants.

The kinetic curves of atrazine adsorption onto SMB650 are shown in Fig. 5, and the parameters of these kinetics models were obtained by regression analysis and listed in Table 2. As can be seen in Table 2, the pseudo second-order model fit the data best with their decision coefficients (R^2) greater than 0.98. The experimental adsorption amounts of atrazine ($q_{e\text{-exp}}$: 930.175, 1110.369 and 1303.006 $\mu\text{g/g}$) were very close to the calculated values ($q_{e\text{-theory}}$) from the pseudo second-order model. Their relative errors were only 5.30%, 5.29% and 6.88%, respectively. Thus, it was more appropriate to describe the adsorption process of atrazine adsorption by the pseudo second-order model. It indicated that both atrazine concentration and SMB650 dosage had influences on

the adsorption behavior under selected conditions [9]. It also indicated that the liquid film diffusion, surface adsorption and intra-particle diffusion might all play a role in the adsorption of atrazine onto SMB650 [28]. In addition, the fitting curve of the intra-particle diffusion model didn't pass through the origin point of coordinate axis ($C \neq 0$), indicating that intra-particle diffusion was not the only dominant rate-controlling step in the adsorption process [29].

Adsorption Isotherms

In order to further reveal the essence of the interactions between adsorbate and adsorbent, batch experiments were performed under different initial atrazine concentrations (1000, 1500, 2000, 2500, 3000 and 4000 $\mu\text{g/L}$) and temperatures (25, 35 and 45°C). The adsorption data was processed by the Langmuir and

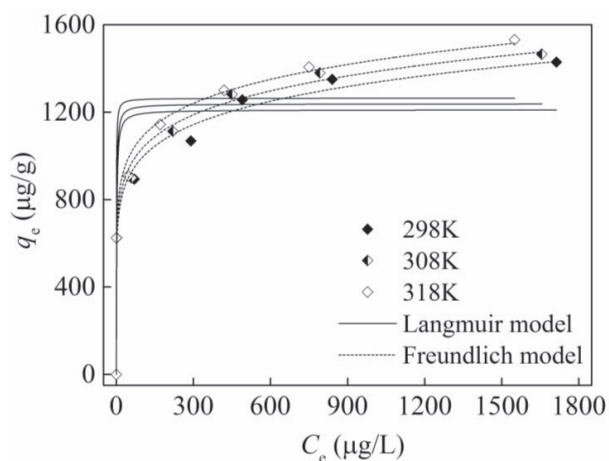


Fig. 6. Adsorption isotherms of atrazine onto SMB650.

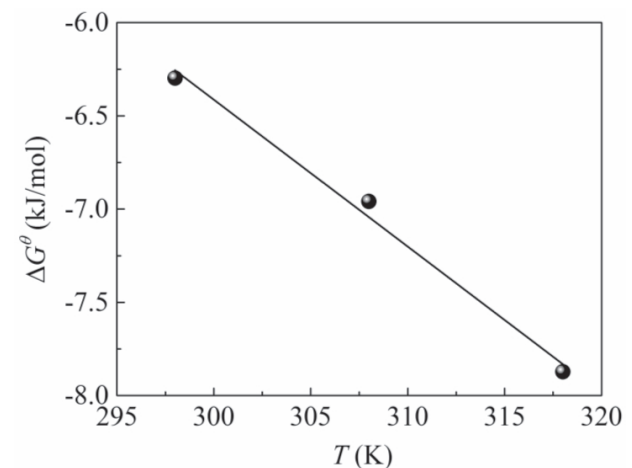
Fig. 7. Relationship between ΔG° and T .

Table 3. Langmuir and Freundlich isotherm parameters for atrazine adsorption.

$T(K)$	Langmuir model			Freundlich model		
	q_m	K_L	R^2	K_F	$1/n$	R^2
298	1 210.527	0.6768	0.8608	546.725	0.1293	0.9891
308	1 237.871	0.9170	0.8579	575.826	0.1269	0.9926
318	1 263.875	2.0371	0.8422	619.518	0.1217	0.9923

Freundlich models. The expressions of Langmuir and Freundlich models can be written as follows:

$$\text{Langmuir model: } q_e = q_m K_L C_e / (1 + K_L C_e) \quad (7)$$

$$\text{Freundlich model: } q_e = K_F C_e^{1/n} \quad (8)$$

...where K_L (L/ μ g) is the Langmuir adsorption equilibrium constant; q_e (μ g/g) is the equilibrium adsorption capacity of adsorbent; q_m (μ g/g) is the theoretical maximum adsorption capacity of adsorbent; C_e (μ g/L) is the concentration of adsorbate at equilibrium; K_F is the adsorption or distribution coefficient of Freundlich model; and $1/n$ is the heterogeneity factor.

The results of atrazine removal were shown in Fig. 6. As could be seen from Fig. 6, the adsorption capacity of SMB650 for atrazine increased with the increase of initial atrazine concentration. This was due to the increase of initial atrazine concentration, leading to the increase of atrazine molecules around the biochar, which augmented the mass transfer power and thus increased the adsorption amount [30]. Besides, the adsorption amount of atrazine by SMB650 increased with the increase of temperature. When the initial ATZ concentration, solution pH and SMB650 dosage were respectively 1500 μ g/L, 3.0 and 1.6 g/L, the ATZ adsorption amounts were 893.538, 900.343 and 908.594 μ g/g with the removal efficiency of 95.3%, 96.0% and 96.9% when the temperatures were respectively 25, 35 and 45°C.

The relevant fitting parameters of Langmuir and Freundlich models are listed in Table 3. According to Table 3, the fitting results of Freundlich model were significantly better than those of Langmuir model, and their decision coefficients (R^2) were all greater than 0.98, indicating that the adsorption behavior of atrazine onto SMB650 was more consistent with the Freundlich model and belonged to the multi-molecular layer adsorption. Based on previous studies [31, 32],

the constant K_F of the Freundlich model represented the quantity of atrazine adsorbed onto SMB650 for unit equilibrium concentration. In this study, the value of K_F rose with the increase of temperature, indicating that the high temperature was favorable to the adsorption. In addition, the constant $1/n$ of the Freundlich model reflected the heterogeneity of adsorption surface. The adsorption process was more difficult to make happen when the value of $1/n$ was greater than 1.0, while the process was comparatively easier when the value of $1/n$ was maintained around 0.1 to 0.5 [33]. In this study, the values of $1/n$ were 0.1293, 0.1269 and 0.1217, respectively, indicating that the adsorption of atrazine onto SMB650 was relatively easy to happen.

Adsorption Thermodynamics

To understand the nature of the adsorption behavior, the thermodynamic parameters for atrazine adsorption onto SMB650 were calculated using the following equations.

$$\Delta G^\theta = \Delta H^\theta - T\Delta S^\theta \quad (9)$$

$$\ln K_d = \Delta S^\theta / R - \Delta H^\theta / RT \quad (10)$$

...where ΔG^θ (kJ/mol), ΔH^θ (kJ/mol) and ΔS^θ [kJ/(mol·K)] stand for the changes of free energy, enthalpy and entropy, respectively; R stands for the ideal gas constant [8.314 J/(mol·K)]; and K_d stands for the thermodynamic equilibrium constant at Kelvin temperature T (K).

The relationship between ΔG^θ and T was shown in Fig. 7, and the thermodynamic parameters for atrazine adsorption on SMB650 are shown in Table 4. The values of ΔG^θ were all negative, indicating that the adsorption process of atrazine onto SMB650 was thermodynamically spontaneous [34, 35]. In addition, the value of ΔG^θ decreased from -6.2976 to -7.8730 kJ/mol as the temperature increased from

Table 4. Thermodynamic parameters for the removal of atrazine by SMB650.

$T(K)$	K_d	ΔG^θ	ΔH^θ	ΔS^θ	R^2
298	12.7031	-6.2976	17.2179	0.0788	0.9830
308	15.1440	-6.9590			
318	19.6453	-7.8730			

298 K to 318 K, representing the fact that higher temperature was favorable to the adsorption reaction [35]. The value of ΔH^θ (17.2179 kJ/mol) was found to be positive, revealing that atrazine adsorption onto SMB650 was an endothermic process [36]. Based on the previous studies [37-39], the higher values of ΔH^θ (>40 kJ/mol) were characteristic of chemical adsorption, while the lower values of ΔH^θ (<25 kJ/mol) indicated that the reaction was physical. Therefore, the adsorption of atrazine onto SMB650 was mainly a physical process. The value of ΔS^θ [0.0788 kJ/(mol·K)] was also positive, confirming that the adsorption was a process of entropy increasing and the degree of chaos between the solid and liquid interface increased [40].

Conclusions

The biochar was prepared by sheep manure at the pyrolysis temperature of 650°C, and its potential to remove atrazine from aqueous solution was investigated using batch experiments. The physicochemical properties of SMB650 showed that it had a good foundation for atrazine adsorption. The adsorption reached equilibrium at 500 min with the atrazine adsorption amount of 893.538 µg/g and the removal efficiency of 95.3% when the initial atrazine concentration, initial solution pH, SMB650 dosage and temperature were respectively 1500 µg/L, 3.0, 1.6 g/L and 25°C. The pseudo second-order and the Freundlich model could more accurately describe the adsorption behavior of atrazine onto SMB650. The calculated thermodynamic parameters indicated that the atrazine adsorption onto SMB650 was a spontaneous and endothermic process. In conclusion, SMB650 was found to be an innovative, efficient and low-cost adsorbent for the removal of atrazine in wastewater.

Acknowledgements

This study was financially supported by the Science and Technology Project of Sichuan Province under grant No. 2017GZ0375, the Key Project of Education Department in Sichuan Province under grant No. 17ZB0031, and the Technology Research and Development Project of Chengdu under grant No. 2015-HM01-00333-SF.

Conflict of Interest

The authors declare no conflict of interest.

References

- THORPE N., SHIRMOHAMMADI A. Herbicides and nitrates in groundwater of Maryland and childhood cancers: A geographic information systems approach. *J. Environ. Sci. Heal C.* **23**, 261, **2005**.
- BARCO-BONILLA N., ROMERO-GONZALEZ R., PLAZA-BOLANOS P., VIDAL J.L.M., FRENICH A.G. Systematic study of the contamination of wastewater treatment plant effluents by organic priority compounds in Almeria province (SE Spain). *Sci. Total Environ.* **447**, 381, **2013**.
- MORENO-GONZALEZ R., CAMPILLO J.A., GARCIA V., LEON V.M. Seasonal input of regulated and emerging organic pollutants through surface watercourses to a Mediterranean coastal lagoon. *Chemosphere.* **92** (3), 247, **2013**.
- SINGH S., KUMAR V., CHAUHAN A., DATTA S., WANI A.B., SINGH N., SINGH J. Toxicity, degradation and analysis of the herbicide atrazine. *Environ. Chem. Lett.* **2**, 1, **2017**.
- LASSERRE J.P., FACK F., SERCHI T., REVETS D., PLANCHON S., RENAUT J., HOFFMANN L., GUTLEB A.C., MULLER C.P., BOHN T. Atrazine and pcb 153 and their effects on the proteome of subcellular fractions of human MCF-7 cells. *Bba-Proteins Proteom.* **1824**, 833, **2012**.
- ZHAO X.C., OUYANG W., HAO F.H., LIN C.Y., WANG F.L., HAN S., GENG X.J. Properties comparison of biochars from corn straw with different pretreatment and sorption behaviour of atrazine. *Bioresource Technol.* **147**, 338, **2013**.
- PAL J., DEB M.K., SIRCAR J.K., AGNIHOTRI P.K. Microwave green synthesis of biopolymer-stabilized silver nanoparticles and their adsorption behavior for atrazine. *Appl. Water Sci.* **5**, 181, **2015**.
- WANG P.F., YIN Y.Y., GUO Y., WANG C. Preponderant adsorption for chlorpyrifos over atrazine by wheat straw-derived biochar: experimental and theoretical studies. *Rsc Adv.* **6**, 10615, **2016**.
- ALAHABADI A., MOUSSAVI G. Preparation, characterization and atrazine adsorption potential of mesoporous carbonate-induced activated biochar (CAB) from Calligonum Comosum biomass: Parametric experiments and kinetics, equilibrium and thermodynamic modeling. *J. Mol. Liq.* **242**, 40, **2017**.
- MOREIRA A.J., BORGES A.C., GOUVEA L.F.C., MACLEOD T.C.O., FRESCHI G.P.G. The process of atrazine degradation, its mechanism, and the formation of metabolites using UV and UV/MW. *J. Photoch. Photobio. A.* **347**, 160, **2017**.
- YANG J.X., LI J., DONG W.Y., MA J., CAO J., LI T.T., LI J.Y., GU J., LIU P.X. Study on enhanced degradation of atrazine by ozonation in the presence of hydroxylamine. *J. Hazard. Mater.* **316**, 110, **2016**.
- CHENG M., ZENG G.M., HUANG D.L., LAI C., XU P., ZHANG C., LIU Y., WAN J., GONG X.M., ZHU Y. Degradation of atrazine by a novel Fenton-like process and assessment the influence on the treated soil. *J. Hazard. Mater.* **312**, 184, **2016**.
- QIU Y.P., ZHENG Z.Z., ZHOU Z.L., SHENG G.D. Effectiveness and mechanisms of dye adsorption on a straw-based biochar. *Bioresource Technol.* **100**, 5348, **2009**.
- YANG G.X., JIANG H. Amino modification of biochar for enhanced adsorption of copper ions from synthetic wastewater. *Water Res.* **48**, 396, **2014**.
- WANG Z.H., SHEN D.K., SHEN F., LI T.Y. Phosphate adsorption on lanthanum loaded biochar. *Chemosphere.* **150**, 1, **2016**.

16. TAN G.C., SUN W.L., XU Y.R., WANG H.Y., XU N. Sorption of mercury (II) and atrazine by biochar, modified biochars and biochar based activated carbon in aqueous solution. *Bioresource Technol.* **211**, 727, **2016**.
17. ZHANG W.H., ZHENG J., ZHENG P.P., Qiu R.L. Atrazine immobilization on sludge derived biochar and the interactive influence of coexisting Pb(II) or Cr(VI) ions. *Chemosphere.* **134**, 438, **2015**.
18. ZHAO L., DONG Y.H., WANG H. Residues of veterinary antibiotics in manures from feedlot livestock in eight provinces of China. *Sci. Total Environ.* **408**, 1069, **2010**.
19. CANG L., WANG Y.J., ZHOU D.M., DONG Y.H. Heavy metals pollution in poultry and livestock feeds and manures under intensive farming in Jiangsu Province, China. *J. Environ. Sci.-China.* **16**, 371, **2004**.
20. XIONG X.O., LI Y.X., LI W., LIN C.Y., HAN W., YANG M. Copper content in animal manures and potential risk of soil copper pollution with animal manure use in agriculture. *Resour. Conserv. Recy.* **54**, 985, **2010**.
21. MANDAL A., SINGH N., PURAKAYASTHA T.J. Characterization of pesticide sorption behaviour of slow pyrolysis biochars as low cost adsorbent for atrazine and imidacloprid removal. *Sci. Total Environ.* **577**, 376, **2017**.
22. FENG D., YU H.M., DENG H., LI F.Z., GE C.J. Adsorption characteristics of norfloxacin by biochar prepared by cassava dreg: kinetics, isotherms, and thermodynamic analysis. *Bioresources.* **10**, 6751, **2015**.
23. QIAN J., SHEN M.M., WANG P.F., WANG C., LI K., LIU J.J., LU B.H., TIAN X. Perfluorooctane sulfonate adsorption on powder activated carbon: Effect of phosphate (P) competition, pH, and temperature. *Chemosphere.* **182**, 215, **2017**.
24. WANG L., CHEN, G.C., LING, C., ZHANG, J.F., SZERLAG, K. Adsorption of Ciprofloxacin on to Bamboo Charcoal: Effects of pH, Salinity, Cations, and Phosphate. *Environ. Prog. Sustain.* **36**, 1108, **2017**.
25. WEI Z.G., LIANG K., WU Y., ZOU Y.D., ZUO J.H., ARRIAGADA D.C., PAN Z.C., HU G.H. The effect of pH on the adsorption of arsenic(III) and arsenic(V) at the TiO₂ anatase [101] surface. *J. Colloid Interf. Sci.* **462**, 252, **2016**.
26. KARA S., AYDINER C., DEMIRBAS E., KOBYA M., DIZGE N. Modeling the effects of adsorbent dose and particle size on the adsorption of reactive textile dyes by fly ash. *Desalination.* **212**, 282, **2007**.
27. YANG S.T., LI J.X., SHAO D.D., HU J., WANG X.K. Adsorption of Ni(II) on oxidized multi-walled carbon nanotubes: Effect of contact time, pH, foreign ions and PAA. *J. Hazard. Mater.* **166**, 109, **2009**.
28. HO Y.S. Review of second-order models for adsorption systems. *J. Hazard. Mater.* **136**, 681, **2006**.
29. EL BOURAIE M., MASOUD A.A. Adsorption of phosphate ions from aqueous solution by modified bentonite with magnesium hydroxide Mg(OH)₂. *Appl. Clay. Sci.* **140**, 157, **2017**.
30. ALJEBOREE A.M., ALKAIM A.F., AL-DUJAILI A.H. Adsorption isotherm, kinetic modeling and thermodynamics of crystal violet dye on coconut husk-based activated carbon. *Desalin. Water Treat.* **53**, 3656, **2015**.
31. ALEMAYEHU E., THIELE-BRUHN S., LENNARTZ B. Adsorption behaviour of Cr(VI) onto macro and micro-vesicular volcanic rocks from water. *Sep. Purif. Technol.* **78**, 55, **2011**.
32. KYZAS G.Z., DELIYANNI E.A., MATIS K.A. Activated carbons produced by pyrolysis of waste potato peels: Cobalt ions removal by adsorption. *Colloid Surface A.* **490**, 74, **2016**.
33. NAMASIVAYAM C., KAVITHA D. Removal of Congo Red from water by adsorption onto activated carbon prepared from coir pith, an agricultural solid waste. *Dyes Pigments.* **54** (1), 47, **2002**.
34. ABIGAIL M.E.A., CHIDAMBARAM R. Rice husk as a low cost nanosorbent for 2,4-dichlorophenoxyacetic acid removal from aqueous solutions. *Ecol. Eng.* **92**, 97, **2016**.
35. MOUSSAVI G., HOSSEINI H., ALAHABADI A. The investigation of diazinon pesticide removal from contaminated water by adsorption onto NH₄Cl-induced activated carbon. *Chem. Eng. J.* **214**, 172, **2013**.
36. ALI I., ALOTHMAN Z.A., AL-WARTHAN A. Sorption, kinetics and thermodynamics studies of atrazine herbicide removal from water using iron nano-composite material. *Int. J. Environ. Sci. Te.* **13**, 733, **2016**.
37. GUPTA V.K., PATHANIA D., SHARMA S., SINGH P. Preparation of bio-based porous carbon by microwave assisted phosphoric acid activation and its use for adsorption of Cr(VI). *J. Colloid Interf. Sci.* **401**, 125, **2017**.
38. LI Y.H., DI Z.C., DING J., WU D.H., LUAN Z.K., ZHU Y.Q. Adsorption thermodynamic, kinetic and desorption studies of Pb²⁺ on carbon nanotubes. *Water Res.* **39**, 605, **2005**.
39. CHOWDHURY S., MISHRA R., SAHA P., KUSHWAHA P. Adsorption thermodynamics, kinetics and isosteric heat of adsorption of malachite green onto chemically modified rice husk. *Desalination.* **265**, 159, **2011**.
40. JOHIR M.A.H., PRADHAN M., LOGANATHAN P., KANDASAMY J., VIGNESWARAN S. Phosphate adsorption from wastewater using zirconium (IV) hydroxide: Kinetics, thermodynamics and membrane filtration adsorption hybrid system studies. *J. Environ. Manage.* **167**, 167, **2016**.